Journal of Zhejiang University SCIENCE A
ISSN 1673-565X (Print); ISSN 1862-1775 (Online)
www.zju.edu.cn/jzus; www.springerlink.com
E-mail: jzus@zju.edu.cn

Traversing the singularity hypersurface by applying the input disturbances to 6-SPS parallel manipulator*

Yu-tong LI†1, Yu-xin WANG[1], Shuang-xia PAN[1], Rui-qin GUO[2]

([1]*College of Mechanical Engineering and Energy, Zhejiang University, Hangzhou 310027, China*)

([2]*Department of Mechanical Engineering, Tongji University, Shanghai 200092, China*)

†E-mail: creativetj@263.com

Received Oct. 20, 2007; revision accepted Apr. 16, 2008

Abstract: The singular points of a 6-SPS Stewart platform are distributed on the multi-dimensional singularity hypersurface in the task-space, which divides the workspace of the manipulator into several singularity-free regions. Because of the motion uncertainty at singular points, while the manipulator traverses this kind of hypersurface from one singularity-free region to another, its motion cannot be predetermined. In this paper, a detailed approach for the manipulator to traverse the singularity hypersurface with its non-persistent configuration is presented. First, the singular point transfer disturbance and the pose disturbance, which make the perturbed singular point transfer horizontally and vertically, respectively, are constructed. Through applying these disturbances into the input parameters within the maximum loss control domain, the perturbed persistent configuration is transformed into its corresponding non-persistent one. Under the action of the disturbances, the manipulator can traverse the singularity hypersurface from one singularity-free region to another with a desired configuration.

Key words: Parallel manipulator, Singularity hypersurface, Singularity-free moving region
doi:10.1631/jzus.A0720034 **Document code:** A **CLC number:** TH11

INTRODUCTION

It is well known that there exist many singularities in the whole workspace for the 6-SPS Gough-Stewart platforms (6-6 SPMs), which lead to loss of rigidity in certain direction(s), and unbounded loads at one or more passive joints. Therefore identification and avoidance of singularities for this kind of manipulator are of practical importance, and they have attracted a significant volume of research.

Identification of the singularity manifold of the 6-6 SPMs is an active area of research. In recent years, researchers have used various computational algebra tools to arrive at the analytical form. St-Onge and Gosselin (1996) used the singularity condition proposed in (Gosselin and Angeles, 1990), and derived a polynomial expression for the singularity manifold of the general SPM. Kim and Chung (1999) used an alternate formulation of the linear velocity relationships to arrive at a similar expression with a less number of terms. St-Onge and Gosselin (2000) refined their earlier work to report the algebraic structure of the singularity manifold of the SPM for various architectural classes. Di Gregorio (2002) presented a new expression of the singularity condition of the most general mechanism based on the mixed products of vectors, and transformed the singularity condition into a ninth-degree polynomial equation whose singularity polynomial equation is cubic in the platform orientation parameters. Huang and Cao (2005) studied the singularity loci and distribution characteristics of the simplified symmetric triangle manipulator architecture, where all singularities are classified into three different linear-complex singularities. Wolf and Shoham (2003) used the line geometry and the screw theory to determine the singular points of parallel manipulators and their behaviors at these points. Li *et al*.(2006) presented an analytic form of the 6D

* Project (Nos. 50375111 and 50675188) supported by the National Natural Science Foundation of China

singularity locus of the general Gough-Stewart platform. When the orientation of the manipulator is given, the type-II singularities (St-Onge and Gosselin, 2000) are distributed on the 3D surfaces in the Descartes coordinate system. Bandyopadhyay and Ghosal (2004) presented a compact closed-form singularity manifold expression of the 6-SPS SPMs. The singularity manifold is obtained as the hypersurface in the task-space, SE(3), on which the wrench transformation matrix for the top platform degenerates.

Because of the existence of the singularity hypersurface, the whole workspace of the manipulator is divided into several independent singularity-free regions. However, the form of the hypersurface depends on the pose parameters of the manipulator. While the pose parameters are changed, the form of the hypersurface will be altered. When the manipulator moves from one singularity-free region to another, the manipulator should traverse the hypersurface with a desired configuration. Due to the motion uncertainty at the singular points which distribute on the hypersurface, after passing through the singular point, the motion of the manipulator is uncertain. With the application of parallel manipulators in some important aspects, such as in the aviation and spaceflight, the motion certainty of parallel manipulators at the vicinity of the singular point has been paid much more attention.

Bandyopadhyay *et al*.(2004) developed a scheme for avoiding singularities of a Stewart platform by restructuring a preplanned path in the vicinity of the singular position. Dasgupta and Mruthyunjaya (2000) presented an algorithm to construct continuous paths within the workspace of the Stewart platform for avoiding singularities. Given two end-poses of the manipulator, the algorithm can find out safe via points and plan a continuous path from the initial pose to the final one. Sen *et al*.(2003) used a variational approach for planning singularity-free paths for parallel mechanisms based on a Lagrangian incorporating both a kinetic energy term and a potential energy term to ensure that the obtained path is short and singularity-free. Dash *et al*.(2003) presented a numerical approach for path planning inside the workspace of parallel mechanisms to avoid singularities. The path is modified to avoid the singular configurations by a local routing method based on Grassmann's line geometry.

The singularity-free path planning method can be utilized to avoid singularities of manipulators with a PTP control requirement when two end-poses of the manipulator belong to the same singularity-free region. However, when the starting point and the ending point belong to different singularity-free regions, no singularity-free path, along which the manipulator can traverse the singularity hypersurface with a desired configuration, can be figured out (Dasgupta and Mruthyunjaya, 2000).

Except the singularity-free path planning method for avoiding the singularities, the determination of singularity-free zones in the workspace of parallel mechanisms (Li *et al*., 2007), and the singularity avoidance method by adding redundant degrees of freedom into the non-redundant manipulator (Choudhury and Ghosal, 2000; Wang and Gosselin, 2004; Kim *et al*., 2005) have been studied.

For letting the manipulator work in the whole workspace with a desired configuration, we studied the possibility for a 3-DOF planar manipulator to pass through singular positions with a desired configuration through adding a disturbing control function (Wang *et al*., 2003) into the system. Taking a plane five-bar linkage as an example, the disturbance function for the mechanism to pass through the singular point was constructed (Wang and Liu, 2004). Under the action of the disturbance function, the configuration curves, which intersect in the singular point while the disturbance is not introduced, are separated. In this way, the mechanism can pass through the singular point with a desired configuration. With the aid of the universal unfolding approach, it is found that all configuration branches converged in the same singular point in the unperturbed system for the semi-regular hexagons 6-SPS Gough-Stewart manipulator (SRHGSMP) (St-Onge and Gosselin, 2000) will be separated in the disturbed system (Wang and Li, 2008). In this paper, based on our previous researches (Wang and Wang, 2005; Wang and Li, 2008), the detailed approach for the manipulator to traverse the singularity hypersurface with a desired configuration is presented.

TYPE-II SINGULARITIES

As shown in Fig.1, the fixed dimensions of the SRHGSMP are: R_1 is the distribution radius of six

spherical joints A_i on the movable platform; R_2 is the distribution radius of six spherical joints $B_i(x_{B_i}, y_{B_i}, z_{B_i})$ on the base. The relative angle between two equilateral triangles formed by joints A_1, A_3, A_5 and joints A_2, A_4, A_6 is α_1, and the relative angle between two equilateral triangles formed by joints B_1, B_3, B_5 and joints B_2, B_4, B_6 is α_2. l_i (i=1, 2, ···, 6) are the lengths of the six extendable legs, which are utilized as independent variables.

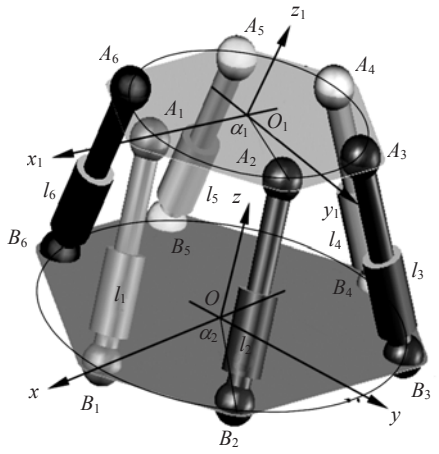

Fig.1 Semi-regular hexagons 6-SPS Gough-Stewart manipulator

The fixed coordinate system $Oxyz$ of the SRHGSMP on the base frame is set up as: the origin of the fixed coordinate system is in the center of the base frame, line OB_1 as x-axis, and the normal line of the fixed frame as z-axis. The movable coordinate system $O_1x_1y_1z_1$ on the movable platform is set up as: line O_1A_1 as x_1-axis, and the normal line of the movable platform as z_1-axis. Joint A_i in the fixed coordinate system is $A_i(x_{A_i}, y_{A_i}, z_{A_i})$, and in the movable coordinate system is $A_i'(x_i', y_i', z_i')$. Utilize $\boldsymbol{X}=[\boldsymbol{P}, \boldsymbol{Q}]^{\mathrm{T}}$ to express the pose of the manipulator, here, $\boldsymbol{P}(x, y, z)$ is the center coordinate parameters of the movable platform, α is the yaw angle of the movable platform with respect to the x-axis, β is the pitch angle of the movable platform with respect to the y-axis, and γ is the roll angle of the movable platform with respect to the z-axis.

According to the length constraint equations for six extensible legs,

$$(\boldsymbol{A}_i-\boldsymbol{B}_i)^{\mathrm{T}}(\boldsymbol{A}_i-\boldsymbol{B}_i)-\boldsymbol{l}_i^{\mathrm{T}}\boldsymbol{l}_i=0,\quad i=1, 2, \cdots, 6, \tag{1}$$

the configuration equations of the SRHGSMP are written as

$$\begin{aligned}\phi_i &= x^2+y^2+z^2+R_1^2+R_2^2-l_i^2+2[x'_{A_i}\cos\beta\cos\gamma\\ &+y'_{A_i}(\sin\alpha\sin\beta\cos\gamma-\cos\alpha\sin\gamma)-x_{B_i}]x\\ &+2[x'_{A_i}\cos\beta\sin\gamma+y'_{A_i}(\sin\alpha\sin\beta\sin\gamma+\cos\alpha\cos\gamma)\\ &-y_{B_i}]y-2(x'_{A_i}\sin\beta-y'_{A_i}\sin\alpha\cos\beta)z-x'_{A_i}y_{B_i}\cos\beta\sin\gamma\\ &+2[-x'_{A_i}x_{B_i}\cos\beta\cos\gamma-y'_{A_i}x_{B_i}(\sin\alpha\sin\beta\cos\gamma\\ &-\cos\alpha\sin\gamma)-y'_{A_i}y_{B_i}(\cos\alpha\cos\gamma+\sin\alpha\sin\beta\sin\gamma)]=0,\\ &i=1, 2, \cdots, 6.\end{aligned} \tag{2}$$

Letting $\boldsymbol{\mu}=[l_1, l_2, \cdots, l_6]^{\mathrm{T}}$, the integrated form of Eq.(2) is

$$\boldsymbol{\Phi}(\boldsymbol{X}, \boldsymbol{\mu})=(\phi_1, \phi_2, \phi_3, \phi_4, \phi_5, \phi_6)^{\mathrm{T}}=\boldsymbol{0}, \tag{3}$$

where $\boldsymbol{\mu}$ is the input parameter vector as independent variables to analyze the configuration bifurcation behaviors; $\boldsymbol{X}$ is a pose vector of the movable platform.

The type-II singularities corresponding to Eq.(3) are determined as follows:

$$\begin{cases}\boldsymbol{\Phi}(\boldsymbol{X}_0, \boldsymbol{\mu}_0)=\boldsymbol{0},\\ \det\left|\partial\boldsymbol{\Phi}(\boldsymbol{X}_0, \boldsymbol{\mu}_0)/\partial\boldsymbol{X}\right|=0.\end{cases} \tag{4}$$

Usually, all six actuators of the manipulator should be driven to give out the outputs, so that the movable platform can move along a specific path in the workspace with given time-varying or static orientation parameters. Because the distribution hypersurface of the type-II singularities has a close relationship with the given orientation parameters, when the orientation parameters are changed, the form of the hypersurface will be alerted. Therefore, in this paper, the input parameters are taken as the independent variables to investigate the configuration bifurcation characteristics of the manipulator.

For the structural semi-symmetry of the manipulator, without loss of universality, select the input parameter l_1 as an independent variable, and keep the other five input parameters constant. When the dimensions of the manipulator are R_1=0.2 m, R_2=0.4 m, α_1=10°, α_2=22°, l_i=0.4 m, i=2, 3, ···, 6, with the homotopy method (Wang and Wang, 2005), from Eq.(3), the configuration bifurcation curves expressed

with the configuration components of the manipulator are drawn in Fig.2.

The determination of the singular points governed by Eq.(4) has some difficulties because while the solution is near the singular points ($\boldsymbol{X}_0$, $\boldsymbol{\mu}_0$), the numerical algorithm becomes unsteady due to the rank reduction of the Jacobian matrix in Eq.(4). In order to eliminate the singularity while solving Eq.(4), the extended equation method (Wu, 1993) is applied. The principle of the extended equation method is that by introducing a new equation to extend the original equation, for instance Eq.(4) here, the rank reduction existed in the original equation is eliminated in the extended equation.

For extending the original equation, the variable set in Eq.(4) should be expanded as $\boldsymbol{\Omega}=(\boldsymbol{X}, \boldsymbol{V}, \boldsymbol{\mu})$ and meet $\boldsymbol{\Phi}(\boldsymbol{X}, \boldsymbol{\mu})=\boldsymbol{0}$. Then construct the extended equation

$$\boldsymbol{\Gamma}(\boldsymbol{\Omega}) := \left\{ \begin{aligned} &\phi_i = \phi_i(x, y, z, \alpha, \beta, \gamma) = 0, \\ &\phi_{jx} = 0,\ \sum_{k=1}^{6} v_k^2 - 1 = 0 \end{aligned} \right\}, \tag{5}$$

where

$$\phi_{jx} = \frac{\partial \phi_j}{\partial x} v_1 + \frac{\partial \phi_j}{\partial y} v_2 + \frac{\partial \phi_j}{\partial z} v_3 + \frac{\partial \phi_j}{\partial \alpha} v_4 + \frac{\partial \phi_j}{\partial \beta} v_5 + \frac{\partial \phi_j}{\partial \gamma} v_6,$$

here, $\boldsymbol{V}=(v_1, v_2, \cdots, v_6)^{\mathrm{T}}$ is the eigenvector corresponding with the zero eigenvalue of the Jacobian matrix of Eq.(4), and $\boldsymbol{\Omega}=(x, y, z, \alpha, \beta, \gamma, v_1, v_2, v_3, v_4, v_5, v_6, l_1, l_2, l_3, l_4, l_5, l_6)^{\mathrm{T}}$.

It can be verified that the solutions of Eq.(5) meet Eq.(4). However, the rank reduction phenomenon due to the rank reduction of the Jacobian matrix in Eq.(4) is eliminated in Eq.(5).

The singular points can be figured out with the numerical algorithm from Eq.(5). The singular points in the above space of the base $z\geq 0$ are listed in Table 1.

Similarly, selecting two or three input parameters as independent variables, letting $l_i=l_j$ (while with two independent variables), or $l_i=l_j=l_k$ (while with three independent variables), and keeping other input parameters constant, the configuration curves going with two and three input parameters have been analyzed. The investigation shows that the configuration curves going with the multi-input parameters are similar with those as shown in Fig.2. Moreover, the

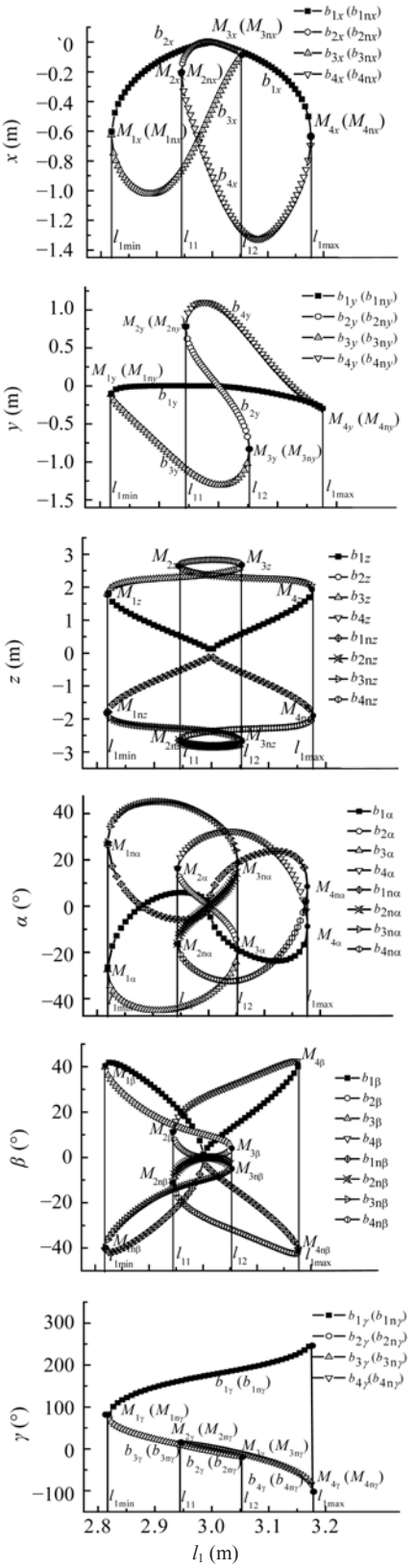

Fig.2 Configuration curves of the SRHGSPM going with input parameter l_1

Table 1 Type-II singular points of the SRHGSPM ($z \geq 0$)

Singular points	l_1	Position			Orientation			Value of Jacobian matrix
		x (m)	y (m)	z (m)	α (°)	β (°)	γ (°)	
M_1	0.31270	0.05930	−0.05818	−0.03682	63.7695	0.1449	−53.1813	-5.238×10^{-13}
M_2	0.35952	−0.01136	−0.09910	0.29714	−17.4806	18.7434	−15.6831	3.652×10^{-11}
M_3	0.42534	0.01290	0.10110	0.31942	22.6161	−6.2082	17.3163	5.972×10^{-10}
M_4	0.47846	−0.00479	0.09896	0.08300	59.6888	15.5147	82.4794	-4.682×10^{-13}

configuration curves for the manipulators with irregularly distributed spherical joints both on the base and on the movable platform have been analyzed. The results show that they are similar with the curves as shown in Fig.2. Therefore, the singularity avoidance method set up based on the configuration curves as shown in Fig.1 can be applied to the singularity avoidance of the manipulator under action of the multiple input parameters.

APPROACH TO TRAVERSE THE SINGULARITY HYPERSURFACE

Traversing the singularity hypersurface

The task-space of the parallel manipulator has been divided into several different singularity-free regions by the singularity distribution hypersurface corresponding to a group of given pose parameters, as shown in Fig.5 in (Bandyopadhyay and Ashitava, 2006). Its projection in one plane can be expressed with Fig.3. In this figure, the configuration along which the manipulator moves close to the singular point is called the persistent configuration, and the corresponding configuration curve is called the persistent configuration curve or branch. The other configuration branch, which intersects with the persistent configuration branch at the singular point, is called the non-persistent configuration branch. The singularity hypersurface denoted with heavy line has divided the workspace into two singularity-free regions: the singularity-free region 1 and the singularity-free region 2.

When the manipulator approaches to the singular point, which is distributed on the singularity hypersurface, it has at least two kinds of configurations to embody: its persistent configuration or non-persistent configuration. Therefore, the motion direction of the manipulator at the singular point is uncertain. To give out a concrete motion within the whole workspace, the manipulator should have the capability to traverse the singularity hypersurface and move from one singularity-free region to another with a desired configuration. Therefore, investigation of the method for the manipulator to traverse the singularity hypersurface with a desired configuration is of important significance for the motion certainty of the manipulator in the whole workspace.

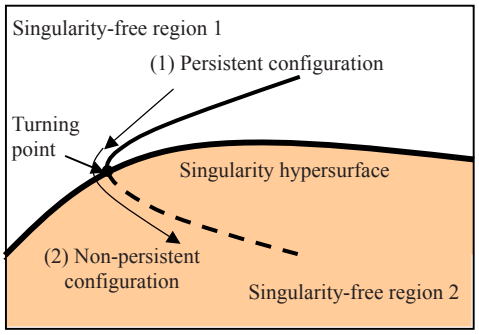

Fig.3 Manipulator traverses the singularity hypersurface

Since the persistent configuration and the non-persistent configuration correspond to the same group of the input parameters, if the manipulator can traverse the singularity hypersurface along the persistent configuration curve and the non-persistent configuration curve before and after traversing the hypersurface, the manipulator can traverse the singularity hypersurface along other configuration curve undoubtedly. The reason is that in the latter case, one group of input parameters has only one configuration to correspond; However, in the former case, one group of input parameters has at lest two configurations to correspond. Comparing with the former case, the latter is relatively simple. Therefore, in this paper, to investigate the approach for the parallel manipulator to traverse the singularity hypersurface, the case that the manipulator moves along the persistent and non-persistent configuration curves before and after traversing the singularity hypersurface is taken as the object.

Maximum loss control domain

A concept of the maximum loss control domain (MLCD) (Wang *et al*., 2005) is elucidated briefly in Fig.4. In this figure, ε is the output precision of the extendable legs, which is guaranteed by the control system, $P_{\mathrm{p}i}$ and $P_{\mathrm{np}i}$ are two points corresponding to ε on the persistent and non-persistent configurations, respectively. When the manipulator arrives to the local zone $l_j \in (l_{jM}, l_{jM}+\varepsilon)$, because the self-motion in this local zone is permitted by the output precision of the system, the manipulator can obtain local free-motion from $P_{\mathrm{p}i}$ to $P_{\mathrm{np}i}$ on the configuration component X_i. Therefore, the motion of the manipulator in this local zone is uncertain. In order to obtain the concrete motion at the vicinity of the singular point, the manipulator should not arrive to the borders defined by points $P_{\mathrm{p}i}$ and $P_{\mathrm{np}i}$, i.e., $S_{\mathrm{b}i}=\min\{S_{\mathrm{p}i}, S_{\mathrm{np}i}\}$ should be greater than ε. Then the MLCD for one component of the configuration is defined as

$$\delta_{1i}=\begin{cases}\left|MP_{\mathrm{p}i}\right|=k\varepsilon, \text{ if } S_{\mathrm{p}i}<S_{\mathrm{np}i},\\ \left|MP_{\mathrm{np}i}\right|=k\varepsilon, \text{ if } S_{\mathrm{p}i}>S_{\mathrm{np}i},\end{cases} \qquad i=1, 2, \cdots, 6, \tag{6}$$

where k>1.5 is a safety coefficient.

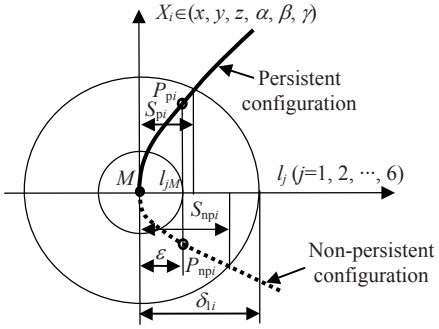

Fig.4 Maximum loss control domain

Then, the MLCD is

$$\delta_1=\max\{\delta_{1i}, i=1, 2, \cdots, 6\}. \tag{7}$$

Obviously, when the manipulator moves beyond the MLCD at the vicinity of the singular point, the motion of the manipulator is concrete. The calculation method for the MLCD had been presented in (Wang *et al*., 2005).

Approach to traverse the singularity hypersurface

It had been found in (Wang and Li, 2008) that all configuration branches converged in the same singular point in the unperturbed system will be separated in the disturbed system while the suitable disturbances are introduced into the system. It gives us a hint to set up a method for the manipulator to traverse the singularity hypersurface. Introducing the disturbances into the extendable legs, i.e., $l_i = l_{iM_j} + \Delta l_i$, it is observed that the negative disturbance (Δl_i<0) and the positive disturbance (Δl_i>0) will cause the perturbed configuration curves and the singular point to move towards the left and the right, respectively. The disturbance which makes the perturbed configuration curves and the singular point move towards the left or the right is called the singular point transfer disturbance.

Generally, the singular point transfer disturbance cannot make sure that the manipulator chooses its non-persistent configuration after ending the disturbance. For the parallel manipulator to traverse the singularity hypersurface with its non-persistent configuration, the pose disturbance should be added. To make the perturbed configuration branch more close to its non-persistent configuration branch, so that the perturbed configuration can be transformed into its non-persistent one within the MLCD.

The approach for the manipulator to traverse the singularity hypersurface is illustrated in Fig.5. In this figure, c_{g} is a given control trace of the configuration of the movable platform, which passes through the singular point M_m, $c_{\mathrm{g}-}$ and $c_{\mathrm{g}+}$ are the persistent configuration curve and the non-persistent configuration curve, respectively. Suppose that the manipulator moves close to the singular point M_m along its $c_{\mathrm{g}-}$. Under the suitable magnitude of the singular point transfer disturbance, the disturbed singular point M_m' moves towards the right with the displacement of the radius of the MLCD δ_1 to M_m''. Then the pose disturbance is applied to guarantee that the perturbed persistent configuration curve $c_{\mathrm{g}-}'$ is more close to its non-persistent configuration curve $c_{\mathrm{g}+}$. In this way, the perturbed persistent configuration curve $c_{\mathrm{g}-}''$ can be transformed into its non-persistent configuration curve $c_{\mathrm{g}+}$. While the persistent configuration curve $c_{\mathrm{g}-}$ is transformed into its non-persistent configuration curve $c_{\mathrm{g}+}$, it means that the persistent configuration of the manipulator has been transformed into its non-persistent one. Therefore, the singularity hypersurface has been traversed.

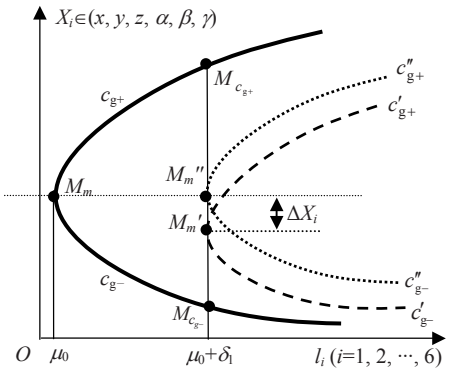

Fig.5 Approach for the manipulator to traverse the singularity hypersurface

DETERMINATION OF DISTURBANCES

Singular point transfer disturbance

1. Input parameter to apply the disturbance

For the sake of decreasing the amplitude of the applied disturbance, the singular point transfer disturbance should be applied to the extendable leg whose length increment is more sensitive to the transitions of the perturbed configuration curves and singular point. For this reason, here, the perturbed sensitive coefficient is defined to express the capability for the disturbance applied to the ith input parameter to shift the singular point. Letting ΔM_{mi} express the displacement of the perturbed singular point M_{mi}' relative to M_m under the disturbance Δl_i applied to the input parameter l_i, then the perturbed sensitive coefficient for ith input parameter is defined as

$$\bar{k}_{m1i} = \Delta M_{mi} / \Delta l_i , \quad i=1, 2, \cdots, 6. \tag{8}$$

The calculation of $\bar{k}_{m1i}$ is as follows. Adding an increment Δl_i ($\Delta l_i > \delta_1$) to the input parameter l_i, and substituting $l_i = l_{iM_m} + \Delta l_i$ for l_i in Eq.(5), with the Newton-Raphson method, we can obtain the new perturbed singular point M_{mi}'. The displacement of the perturbed singular point M_m' is $\Delta M_{mi}' = M_{mi}' - M_m$. For instance, the perturbed sensitive coefficients corresponding to the different input parameters at the singular point M_2 are listed in Table 2. In this table, the positive value means that the positive disturbance applied to the input parameter l_2 will lead the perturbed singular point M_{22}' to move towards the right, the negative value in reverse. It is obvious that the disturbance applied to the second input parameter is the most sensitive one to shift the singular point M_2. Therefore, it is an idea to apply the disturbance to the second input parameter l_2.

The perturbed sensitive coefficient set relative to Table 2 is

$$\sum k_{m1} = \left\{ \bar{k}_{m1i} \in R \,||\, \Delta l_1 | \le \varepsilon \right\}, \ i=2, 3, \cdots, 6. \tag{9}$$

Table 2 Perturbed sensitive coefficients (PSC) at the singular point M_2

PSC	Value	PSC	Value
$\bar{k}_{212}$	1.27	$\bar{k}_{215}$	0.83
$\bar{k}_{213}$	0.05	$\bar{k}_{216}$	−0.714
$\bar{k}_{214}$	0.02		

2. Amplitude of the singular point transfer disturbance

The steps to calculate the singular point transfer disturbances are as follows:

(1) Make certain of the transfer direction of the singular point, in which the perturbed persistent configuration branch is close to the non-persistent configuration branch. For instance, at the singular point M_2, the direction is towards the right.

(2) Figure out the maximum perturbed sensitive coefficient, $\bar{k}_{m1j} = \max_i \{\bar{k}_{m1i}\}$, $i = 1, 2, \cdots, 6$, based on Eq.(9), and apply the disturbance to the input parameter l_j. At the singular point M_2, from Table 2, the singular point transfer disturbance should be applied to the input parameter l_2.

(3) Determine the amplitude of the disturbance. For the precision of the input parameters ε, determine the radius of the MLCD δ_1 based on the calculation approach supplied by (Wang *et al*., 2005). The amplitude of the applied disturbance to the input parameter l_j should meet

$$\Delta l_{m1} = \frac{\delta_1}{\bar{k}_{m1j}} > \varepsilon. \tag{10}$$

The above inequality is utilized to guarantee that the perturbed singular point locates beyond the radius of the MLCD δ_1 corresponding to the singular point. For instance, as shown in Fig.5, the distance between M_m and M_m' should be greater than the radius of the MLCD δ_1.

Pose disturbances

1. Pose component to apply disturbance

Similarly, for reducing the amplitude of the disturbance, the pose disturbance should be applied to this kind of component of the configuration: within the MLCD, if the disturbance applied to the component leads it to convert from its perturbed persistent configuration to its non-persistent one, the other components will be certainly transformed from their perturbed persistent configurations to their non-persistent ones, respectively.

For choosing the component of the configuration to apply the disturbance, the configuration convert coefficients are defined here. Suppose that $M_{c_{g-}}$ and $M_{c_{g+}}$ are two intersecting points of the two configuration branches (persistent one and non-persistent one) with the boundary line relative to the MLCD, as shown in Fig.5. Obviously, the smaller the distance between $M_{c_{g-}}$ and $M_{c_{g+}}$, the easier the component converts from its persistent configuration c_{g-} to its non-persistent configuration c_{g+}. Thus, the configuration convert coefficients are defined as Eq.(11):

$$\eta_{X_i}=\frac{\left|X_{ic_{g-}}-X_{ic_{g+}}\right|}{\sqrt{(x_{c_{g-}}-x_{c_{g+}})^2+(y_{c_{g-}}-y_{c_{g+}})^2+(z_{c_{g-}}-z_{c_{g+}})^2}},\quad X_i\in(x,y,z);$$

$$\eta_{X_i}=\frac{\left|X_{ic_{g-}}-X_{ic_{g+}}\right|}{\sqrt{(\alpha_{c_{g-}}-\alpha_{c_{g+}})^2+(\beta_{c_{g-}}-\beta_{c_{g+}})^2+(\gamma_{c_{g-}}-\gamma_{c_{g+}})^2}},\quad X_i\in(\alpha,\beta,\gamma). \tag{11}$$

The configuration convert coefficients have reflected the extents for one configuration component to convert from its persistent configuration to its non-persistent one. The numerical analysis shows that when the pose disturbance is applied to the fourth ascending order component, usually, all six components of the configuration will be converted from their persistent configurations to their non-persistent ones.

2. Amplitude of pose disturbance

The pose disturbance should make the disturbed persistent configuration more close to its non-persistent one. The mathematical condition of this requirement is shown in Eq.(12):

$$\left|X_{ic''_{g-}}-X_{ic_{g+}}\right|\le\frac{1}{2}\left|X_{ic_{g-}}-X_{ic_{g+}}\right|,\ l_1\in(l_{1M_m},l_{1M_m}+\varepsilon). \tag{12}$$

The steps to determine the pose disturbance are:

(1) Calculate the position of the disturbed singular point M_m' under the singular point transfer disturbance.

Applying the singular point transfer disturbance $\Delta l_j=\delta_1/\bar{k}_{m1j}>\varepsilon$ to the input parameter l_j, letting $l_j=l_{jM_m}+\Delta l_j$, here l_{jM_m} is the value of l_j at the singular point M_m, and substituting it into Eq.(5), then, we can obtain the disturbed singular point M_m' (such as M_{20}' in Fig.5). Since the MLCD belongs to the germ space, the disturbed singular point M_m' is usually at the boundary of the MLCD relative to the undisturbed singular point M_m.

(2) Determine the pose component X_i to apply the pose disturbance according to the ascending order of the configuration convert coefficients determined by Eq.(11). Let M_m'' be an intersecting point of the symmetrical line of the persistent configuration and the non-persistent one with the boundary line of the MLCD, then, the amplitude of the applied pose disturbance is $\Delta X_i=M_m'-M_m''$.

(3) Calculate the perturbed increment for each input parameter corresponding to ΔX_i.

Suppose that the inverse kinematics for the parallel manipulator is

$$l_n=\mu_n(x,y,z,\alpha,\beta,\gamma),\ n=1,2,\cdots,6. \tag{13}$$

The perturbed increments for each input parameter corresponding to ΔX_i are

$$\Delta l_n=\frac{\partial\mu_n}{\partial X_i}\Delta X_i=\bar{k}_{m2n}\Delta X_i,\ n=1,2,\cdots,6. \tag{14}$$

$\bar{k}_{m2n}$ in Eq.(14) is called the pose disturbance sensitive coefficient. And it should meet Eq.(15):

$$\sum k_{m2}=\left\{\bar{k}_{m2n}\Delta X_i\in R\left|\left|X_{ic''_{g-}}-X_{ic_{g+}}\right|\le\frac{1}{2}\left|X_{ic_{g-}}-X_{ic_{g+}}\right|\right.\right\},\quad X_i\in(x,y,z,\alpha,\beta,\gamma). \tag{15}$$

Procedure to construct the disturbance function

According to the configuration curves going with the single input parameter, as shown in Fig.2, in the above space of the based, there are four singular points. The configuration bifurcation behaviors at the singular point M_1 are similar with those at the singular point M_2, and the configuration bifurcation behaviors at the singular point M_3 are similar with those at the singular point M_4. Therefore, if the construction of the disturbance function at one singular point, such as at the singular point M_2, is mastered, the disturbance function at other singular points can be constructed similarly. The procedure to construct the disturbance functions at singular points is listed in Table 3.

EXAMPLE

Here take the singular point M_2 as an example to illustrate the approach to construct the disturbance functions. In this example, the manipulator is close to the singular point M_2 along the configuration curve b_3. After passing through the singular point, the manipulator should move along its non-persistent configuration b_7.

Disturbance functions

1. Turning point transfer disturbance function

According to Table 2, the disturbance applied to the input parameter l_2 is the most sensitive one to the transition of the perturbed configuration curves and singular point. Therefore, the singular point transfer disturbance should be applied to the input parameter l_2. When the output precision of the input parameters, which is guaranteed by the control system of the parallel manipulator, is ε=0.0001 m, the radius of the MLCD calculated based on (Wang *et al*., 2005) is δ_1=0.001 m. Based on Eq.(10), the minimum amplitude of the singular point transfer disturbance applied to the extendable leg l_2 is

$$\Delta l_{21}=\frac{\delta_1}{\bar{k}_{212}}=0.000787>\varepsilon. \tag{16}$$

Then, the linear disturbance function is

$$l_{21i}=f_{21}(l_2)=\begin{cases}\left(1-\dfrac{l_1-l_{11}}{\delta_1}\right)\dfrac{\delta_1}{\bar{k}_{212}}, & i=2,\\ 0, & i=1,3,4,5,6.\end{cases} \tag{17}$$

2. Pose disturbance function

Based on Eq.(11), the configuration convert coefficients at the singular point M_2 are calculated and listed in Table 4.

Table 3 The procedure to construct the disturbance functions at M_m, $m\in$(1, 2, 3, 4)

Goal	Procedure
Determining the singular point transfer disturbance	(1) Make certain of the transfer direction of the singular point, in which the perturbed persistent configuration branch is close to the non-persistent configuration branch; (2) Figure out the maximum perturbed sensitive coefficient: $\bar{k}_{m1j}=\max_i\{\bar{k}_{m1i}\}$, i=1, 2, ..., 6, based on Eq.(9); (3) Determine the amplitude of the disturbance applied to the input parameter l_j: $\Delta l_{m1}=\delta_1/\bar{k}_{m1j}>\varepsilon$
Determining the pose disturbances	(4) Calculate the position of the disturbed singular point M_m' under the singular point transfer disturbance; (5) Calculate the configuration convert coefficients determined by Eq.(11), and the pose disturbance is applied to the fourth ascending order component; (6) Calculate the amplitude of the applied pose disturbance according to Eq.(12): $\Delta X_i=M_m'-M_m''$; (7) Calculate the pose disturbance sensitive coefficients based on Eq.(13): $\bar{k}_{m2n}=\partial\mu_n/\partial X_i$, $n=1,2,\cdots,6$; (8) Figure out the pose disturbances applied to each input parameters: $\Delta l_n=\bar{k}_{m2n}\Delta X_i, n=1,2,\cdots,6$, based on Eq.(14)
Constructing linear disturbance functions	(9) Construct linear disturbance functions based on Eq.(15): $l_n=\left(1-\dfrac{l_1-l_{1M_m}}{\delta_1}\right)\bar{k}_{m2n}\Delta X_i+\left\{\left(1-\dfrac{l_1-l_{1M_m}}{\delta_1}\right)\dfrac{\delta_1}{\bar{k}_{m1j}}\right\}_{n=j}$, $n=1,\ 2,\ ...,\ 6$

Table 4 Configuration convert coefficients at the singular point M_2^*

l_1 (m)	η_x	η_y	η_z	η_α	η_β	η_γ
0.4895	0.6065	0.7307	0.3136	0.6769	0.7226	0.1401

*R_1=1 m, R_2=2 m, α_1=50°, α_2=20°, l_i=2.0 m, ε=0.0001 m, δ=0.001 m

The ascending order of the configuration convert coefficients at the singular point M_2 is

$$\eta_\gamma<\eta_z<\eta_x<\eta_\alpha<\eta_\beta<\eta_y. \tag{18}$$

From this ascending order, the pose disturbance should be applied to the component α. The amplitude of the applied pose disturbance $\Delta X_i=M_k'-M_k''$ corresponding to the component α is $\Delta\alpha$=0.40201584°. Based on Eqs.(13) and (14), the pose disturbance sensitive coefficients $\bar{k}_{22n}$ (n=1, 2, ···, 6) corresponding to $\Delta\alpha$ at the singular point M_2 are listed in Table 5.

Table 5 $\bar{k}_{22n}$ (n=1, 2, ···, 6) corresponding to $\Delta\alpha$ at the singular point M_2

$\bar{k}_{22n}$	Value	$\bar{k}_{22n}$	Value
$\bar{k}_{211}$	0	$\bar{k}_{214}$	0.0342
$\bar{k}_{212}$	0.0228	$\bar{k}_{215}$	−0.0400
$\bar{k}_{213}$	0.0570	$\bar{k}_{216}$	−0.0420

The intention of $\bar{k}_{221}=0$ in Table 5 is for guaranteeing that the perturbed singular point is on the boundary of the MLCD corresponding to the singular point M_2.

While $\bar{k}_{224}=0.0342$ and $\alpha'_{b3}=12.3409$

$$\left|\alpha'_{b3}-\alpha_{b7}\right|=2.914<\left|(\alpha_{b3}-\alpha_{b7})/2\right|=3.124, \tag{19}$$

which means that Eq.(12) can be met.

Similarly, the linear pose disturbance functions applied to the input parameters relative to $\Delta\alpha$ are

$$l_{22n}=f_{22}(l_1)=\left(1-(l_1-l_{11})/\delta_1\right)\bar{k}_{22n}\Delta\alpha,\quad n=1,2,3,4,5,6. \tag{20}$$

3. Integrated disturbance functions

According to Eqs.(17) and (20), the integrated disturbance function is

$$\begin{aligned} l_n &= l_{22n}+l_{21n}\\ &=\left(1-\frac{l_1-l_{11}}{\delta_1}\right)\bar{k}_{22n}\Delta\alpha+\left\{\left(1-\frac{l_1-l_{11}}{\delta_1}\right)\frac{\delta_1}{\bar{k}_{212}}\right\}_{n=2},\\ &\qquad n=1,\ 2,3,4,5,6. \end{aligned} \tag{21}$$

Trace for manipulator to traverse the singularity hypersurface

1. Universal unfolding equation of the perturbed system

Supposing that $(\boldsymbol{X}_0, \boldsymbol{\rho}_0)$ is a singular point, letting $\bar{\boldsymbol{X}}=\boldsymbol{X}-\boldsymbol{X}_0$, $\bar{\boldsymbol{\rho}}=\boldsymbol{\rho}-\boldsymbol{\rho}_0$, and with $\boldsymbol{X}$ and $\boldsymbol{\rho}$ to express $\bar{\boldsymbol{X}}$ and $\bar{\boldsymbol{\rho}}$, respectively, then we can obtain the configuration bifurcation equation at the vicinity of the singular point corresponding to the configuration Eq.(3) as follows:

$$\begin{aligned} f_i &= x^2+y^2+z^2+c_{1i}x+c_{2i}y+c_{3i}z-c_{64i}l_i-l_i^2\\ &\quad+c_{0i}+\sum_{j=1}^{6}[c_{(3+j)i}+c_{(9+j)i}z]\upsilon_j\\ &\quad+\sum_{k=1}^{16}[c_{(15+k)i}+c_{(31+k)i}x+c_{(47+k)i}y]\omega_k=0,\\ &\qquad i=1,2,\cdots,6, \end{aligned} \tag{22}$$

where,

$$\begin{aligned} \boldsymbol{\upsilon}&=\{\upsilon_j\}_{j=1,2,\cdots,6}=\{\cos\beta,\ \cos\alpha\cos\beta,\\ &\quad \sin\alpha\cos\beta,\ \sin\beta,\ \cos\alpha\sin\beta,\ \sin\alpha\sin\beta\}^{\mathrm{T}},\\ \boldsymbol{\omega}&=\{\omega_k\}_{k=1,2,\cdots,16}=\{\cos\alpha\cos\gamma,\cos\beta\cos\gamma,\\ &\quad \cos\alpha\cos\beta\cos\gamma,\sin\alpha\cos\gamma,\ \sin\alpha\cos\beta\cos\gamma,\\ &\quad \sin\beta\cos\gamma,\ \cos\alpha\sin\beta\cos\gamma,\ \sin\alpha\sin\beta\cos\gamma,\\ &\quad \cos\alpha\sin\gamma,\cos\beta\sin\gamma,\ \sin\alpha\cos\beta\sin\gamma,\ \sin\beta\sin\gamma,\\ &\quad \cos\alpha\sin\beta\sin\gamma,\sin\alpha\sin\beta\sin\gamma,\cos\alpha\cos\beta\sin\gamma,\\ &\quad \sin\alpha\sin\gamma\}^{\mathrm{T}}, \end{aligned}$$

and c_{mi} (m=0, 1, 2, ···, 64) are the constants relative to the dimensions of the mechanism. l_i are the output increments of six extensible legs at the vicinity of the singular point.

According to the universal unfold theory (Chen and Leung, 1998), while the disturbances are introduced into the system expressed with Eq.(21), the universal unfold equation corresponding to Eq.(22) is

$$f_n=x^2+y^2+z^2+\sum_{j=1}^{6}[c_{(3+j)n}+c_{(9+j)n}z]\upsilon_j$$

$$+\sum_{k=1}^{16}[c_{(15+k)n}+c_{(31+k)n}x+c_{(47+k)n}y]\omega_k$$
$$-c_{64n}\left[\left(1-\frac{l_1-l_{1M_m}}{\delta_1}\right)\overline{k}_{m2n}\Delta\alpha+\left\{\left(1-\frac{l_1-l_{1M_m}}{\delta_1}\right)\frac{\delta_1}{\overline{k}_{m1j}}\right\}_{n=1}\right]$$
$$+c_{1n}x+c_{2n}y+c_{3n}z$$
$$-\left[\left(1-\frac{l_1-l_{1M_m}}{\delta_1}\right)\overline{k}_{m2n}\Delta\alpha+\left\{\left(1-\frac{l_1-l_{1M_m}}{\delta_1}\right)\frac{\delta_1}{\overline{k}_{m1j}}\right\}_{i=n}\right]^2$$
$$+c_{0n}+g_n=0,\quad n=1,2,\cdots,6, \tag{23}$$

where

$$\begin{aligned}g_n=2[&y'_{A_n}(\cos\alpha\sin\beta\cos\gamma+\sin\alpha\sin\gamma)x\\&+y'_{A_n}(\cos\alpha\sin\beta\sin\gamma-\sin\alpha\cos\gamma)y\\&+y'_{A_n}z\cos\alpha\cos\beta-(\cos\alpha\sin\beta\cos\gamma\\&+\sin\alpha\sin\gamma)y'_{A_n}x_{B_n}+(\sin\alpha\cos\gamma\\&-\cos\alpha\sin\beta\sin\gamma)y'_{A_n}y_{B_n}]\overline{k}_{m2n}\Delta X_i.\end{aligned}$$

Eq.(23) is utilized to figure out the perturbed configuration curves.

2. Figure out the disturbance values to be applied at each trace point

Since the MLCD is very small, and the integrated disturbance functions belong to linear functions, the displacement of the singular point M_2 caused by the singular point transfer disturbance can be linearly divided corresponding to the singular point transfer disturbance. Similarly, the displacement of the singular point M_2 caused by the pose disturbances can be linearly divided corresponding to the pose disturbances. For this consideration, the integrated disturbance is equally divided into three (or other number) portions corresponding to $\Delta\alpha_k=k\Delta\alpha/3$, k=1, 2, 3.

Under the disturbances applied to the input parameters, which are

$$\Delta l_{nk}=\left(1-\frac{l_1-l_{11}}{\delta_1}\right)\overline{k}_{22n}\Delta\alpha_k+\left\{\left(1-\frac{l_1-l_{11}}{\delta_1}\right)\frac{\delta_1}{\overline{k}_{212}}\right\}_{n=2},$$
$$n=1,2,\cdots,6;\ k=1,2,3,4, \tag{24}$$

and listed in Table 6, the perturbed singular points will be transferred from M_2 (M_{21}) to M_{22}, M_{23} and M_{24} in turn. Based on the universal unfold Eq.(23), the perturbed configuration curves under the disturbances of Eq.(24) can be figured out then. Similarly, the perturbed trace points from N_1 to N_2, N_3, and to M_{24} under the disturbances of Eq.(24) can be obtained by solving Eq.(23). The perturbed configuration curves b_{3k} (k=1, 2, 3, 4) and the perturbed trace points are drawn in Fig.6.

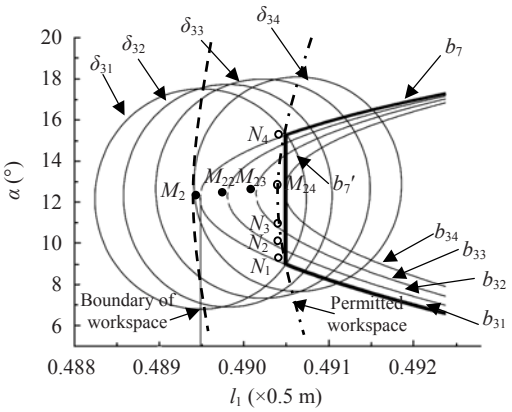

Fig.6 Traces for the manipulator to pass through the singular point with its non-persistent configuration

Since the perturbed process takes place in a very small domain, all of the nonlinear functions can be linearized. Then the perturbed trace points can be considered as the combinations of the singular point transfer disturbance and the pose disturbances. The singular point transfer disturbance makes the perturbed trace point move towards the right horizontally with the distance $\delta_1 k/3$, k=1, 2, 3. However, the pose disturbances make the perturbed trace point move towards the left horizontally with the distance $k/(3|M_{24}M_2|_{\text{horizontal}})$, k=1, 2, 3, and move upwards with the distance $k/(3|M_{24}N_1|_{\text{vertical}})$, k=1, 2, 3. The displacement $\delta_1 k/3$, k=1, 2, 3 and the displacement $k/(3|M_{24}M_2|_{\text{horizontal}})$, k=1, 2, 3 are nearly equal but in

Table 6 Disturbance values applied for each extendable leg

Serial No.	Moving point	Disturbance values applied to each extendable leg					
		Δl_1	Δl_2	Δl_3	Δl_4	Δl_5	Δl_6
1	N_1	0	0	0	0	0	0
2	N_2	0	0.00016	0.00040	0.00024	−0.00028	−0.00030
3	N_3	0	0.00036	0.00091	0.00055	−0.00064	−0.00067
4	M_{24}	0	0.00059	0.00158	0.00096	−0.00104	−0.00106
5	N_4	0	0	0	0	0	0

reverse directions. Therefore, the perturbed trace point moves upwards almost.

3. Traces pass through the singular point with non-persistent configuration

When the manipulator moves along branch b_{31} close to N_1, which is an intersect point of the circle centered at the singular point M_2 with the radius of the MLCD δ_1, the integrated disturbance functions corresponding to Eq.(24) are applied to the input parameters respectively. Under the actions of the disturbances, the manipulator will pass through points N_2, N_3 until to the perturbed singular point M_{24} in turn. Simultaneously, the persistent configuration branch b_3 is converted gradually from b_{31} to b_{32}, b_{33}, until to b_{34}. Since the perturbed trace b_{34} goes through the perturbed singular point M_{24}, when the manipulator moves to this perturbed singular point M_{24}, the configuration of the manipulator has been transformed from its original configuration to its non-persistent one entirely. After the manipulator passes through this point, the input disturbance is removed and only the pose disturbance is applied. Then, the perturbed configuration is transformed from the perturbed trace b_7' to its non-persistent configuration branch b_7. The numerical analysis shows that based on the principle of the minimum potential energy, the manipulator has a tendency to convert its perturbed configuration from b_7' to b_7 by itself, even the pose disturbance is removed after the manipulator passes through the perturbed singular point M_{24}.

Since points N_1, N_2, N_3, M_{24} locate within the MLCD corresponding to the singular point M_2, while the manipulator passes through these points, the motion of the manipulator is uncertain. The uncertain motion at these points is utilized to fulfill the configuration transformation from its perturbed persistent configuration to its non-persistent one. After ending the disturbance, the perturbed persistent configuration has been converted into its non-persistent one, and then the manipulator traverses the singularity hypersurface with the desired configuration.

Because the configuration transformation from the perturbed persistent configuration to its non-persistent one takes place within the MLCD, and during this process the motion of the movable platform is uncertain, it is suggested that the pose of the manipulator should not be programmed strictly during this configuration transformation process. It would be better to program the pose of the manipulator before and after the disturbance process.

4. Method to reduce the deviation caused by the configuration transformation

Comparing with the undisturbed system, the component error on α at M_2 is 6.2496° as shown in Fig.6. This error is too large to be accepted. The deviation depends on two factors: the curvature radius of the configuration curve at the singular point and the radius of the MLCD. The larger the radius curvature, the larger the component deviation. For the parallel manipulator, the configuration curves are decided. Therefore, the possible approaches to reduce the component deviation are:

(1) Reducing the radius of the MLCD by increasing the control precision of the extendable legs will lead the component deviations to decrease dramatically. For instance, in Fig.6, the deviation for the component α is 6.2496° while δ_1=0.001 m. If δ_2=0.0001 m, the deviation is reduced to 2.0052°.

(2) Since the larger the radius curvature of the configuration curve at singular point, the larger the component deviation, the disturbances should be applied to the configuration component whose curvature radius of the configuration curve at singular point are smaller than the others. In this way, the deviations can be reduced.

(3) If the disturbance must be applied to the component whose curvature radius of the configuration curve is larger than the others, this component should be free-programmed at the vicinity of the singular point. The free-programming means that the component is programmed within a certain scope rather than with a single value. Usually, not all of the orientation parameters of the parallel manipulator are needed to be programmed strictly, e.g., the task of the virtual-type tools. Therefore, the free-programming pose strategy can be applied in the trajectory programming of the parallel manipulator. If the deviations on some components are within the permitted variation scopes, these deviations will not influence the output of the parallel manipulator. Obviously, applying the disturbances to the free-programmed components and letting the deviations within the permitted variation scopes will lead the manipulator to pass through the singular point with its non-persistent configuration without influencing the desired output of the parallel manipulator.

CONCLUSION

In this paper, the approach for the manipulator to pass through the singularity hypersurface is presented. This method is based on the discovery that the disturbances applied to the input parameters can make the perturbed singular point and the configuration curves transfer. By applying the singular point transfer disturbance and the pose disturbance, the perturbed persistent configuration is transformed into its non-persistent one within the MLCD. In this way, the manipulator can traverse the singularity hypersurface with a desired configuration.

The deviations of the configuration transformation from the perturbed persistent configuration to its non-persistent one within the MLCD can be reduced by increasing the precision of the control system and by the free-programming pose approach.

References

Bandyopadhyay, S., Ashitava, G., 2006. Geometric characterization and parametric representation of the singularity manifold of a 6-6 Stewart platform manipulator. *Mechanism and Machine Theory*, **41**(11):1377-1400. [doi:10.1016/j.mechmachtheory.2005.12.006]

Bandyopadhyay, S., Ghosal, A., 2004. Analysis of configuration space singularities of closed-loop mechanisms and parallel manipulators. *Mechanism and Machine Theory*, **39**(5):519-544. [doi:10.1016/j.mechmachtheory.2003.08.003]

Chen, Y.S., Leung, A.Y.T., 1998. Bifurcation and Chaos in Engineering. Springer-Verlag, London, p.112-127.

Choudhury, P., Ghosal, A., 2000. Singularity and controllability analysis of parallel manipulators and closed-loop mechanisms. *Mechanism and Machine Theory*, **35**(10):1455-1479. [doi:10.1016/S0094-114X(00)00003-3]

Dasgupta, B., Mruthyunjaya, T.S., 2000. The Stewart platform manipulator: a review. *Mechanism and Machine Theory*, **35**(1):15-40. [doi:10.1016/S0094-114X(99)00006-3]

Dash, A.K., Chen, I.M., Yao, S.H., Yang, G.L., 2003. Singularity-free Path Planning of Parallel Manipulators Using Clustering Algorithm and Line Geometry. IEEE International Conference on Robotics and Automation, ICRA, Taipei, Taiwan, September 14-19.

Di Gregorio, R., 2002. Singularity-locus expression of a class of parallel mechanisms. *Robotica*, **20**(3):323-328. [doi:10.1017/S026357470100399X]

Gosselin, C., Angeles, J., 1990. Singularity analysis of closed loop kinematic chains. *IEEE Transactions on Robotics and Automation*, **6**(3):281-290. [doi:10.1109/70.56660]

Huang, Z., Cao, Y., 2005. Property identification of the singularity loci of a class of Gough-Stewart manipulator. *International Journal of Robotics Research*, **24**(8):675-685. [doi:10.1177/0278364905054655]

Kim, D., Chung, W., 1999. Analytic singularity equation and analysis of six-DOF parallel manipulators using local structurization method. *IEEE Transactions on Robotics and Automation*, **15**(4):612-622. [doi:10.1109/70.781965]

Kim, W.H., Lee, H.J., Suh, H., Yi, B.J., 2005. Comparative study and experimental verification of singular-free algorithms for a 6 DoF parallel haptic device. *Mechatronics*, **15**(4):403-422. [doi:10.1016/j.mechatronics.2004.10.005]

Li, H.D., Gosselin, C.M., Richard, M.J., St-Onge, B.M., 2006. Analytic form of the six-dimensional singularity locus of the general Gough-Stewart platform. *Journal of Mechanical Design*, **128**(1):279-287. [doi:10.1115/1.2118 733]

Li, H.D., Gosselin, C.M., Richard, M.J., 2007. Determination of the maximal singularity-free zones in the six-dimensional workspace of the general Gough-Stewart platform. *Mechanism and Machine Theory*, **42**(4):497-511. [doi:10.1016/j.mechmachtheory.2006.04.006]

Sen, S., Dasgupta, B., Mallik, K.A., 2003. Variational approach for singularity-free path-planning of parallel manipulators. *Mechanism and Machine Theory*, **38**(11):1165-1183. [doi:10.1016/S0094-114X(03)00065-X]

St-Onge, B.M., Gosselin, C., 1996. Singularity analysis and representation of spatial six-DOF parallel manipulators. *Recent Advances in Robot Kinematics*, **2**(3):389-398.

St-Onge, B.M., Gosselin, C., 2000. Singularity analysis and representation of the general Gough-Stewart platform. *International Journal of Robotics Research*, **19**(3):271-288. [doi:10.1177/02783640022066860]

Wang, J., Gosselin, M.C., 2004. Kinematic analysis and design of kinematically redundant parallel mechanisms. *Journal of Mechanical Design*, **126**(1):109-118. [doi:10.1115/1.1641189]

Wang, Y.X., Li, Y.T., 2008. Disturbed configuration bifurcation characteristics of Gough-Stewart parallel manipulators at singular points. *Journal of Mechanical Design*, **130**(2):1-9. [doi:10.1115/1.2813784]

Wang, Y.X., Liu, X.S., 2004. Study on the configuration bifurcation characteristics of the five-bar linkage. *Chinese Journal of Mechanical Engineering*, **40**(11):17-20.

Wang, Y.X., Wang, Y.M., 2005. Configuration bifurcations analysis of six degree-of-freedom symmetrical Stewart parallel mechanisms. *Journal of Mechanical Design*, **127**(1):70-77. [doi:10.1115/1.1814651]

Wang, Y.X., Wang, Y.M., Liu, X.S., 2003. Bifurcation property and persistence of configurations for parallel mechanisms. *Science in China* (*Series E*), **33**(1):1-9.

Wang, Y.X., Wang, Y.M, Chen, Y.S., Huang, Z., 2005. Research on loss of controllability of Stewart parallel mechanisms at bifurcation points. *Chinese Journal of Mechanical Engineering*, **41**(7):40-49.

Wolf, A., Shoham, M., 2003. Investigation of parallel manipulators using linear complex approximation. *Journal of Mechanical Design*, **125**(3):564-572. [doi:10.1115/1.1582876]

Wu, W., 1993. The Expending Method for Solving Nonlinear Bifurcation Problem. Science Publish House, Beijing, p.41-56.